JOURNAL OF Applied Polymer SCIENCE

Characterization of Antireflective Coatings on Poly(methyl methacrylate) Substrate by Different Process Parameters

Wei-Ming Chiu,[1] Yuan-Shun Zhang,[1] Peir-An Tsai,[2] Jyh-Horng Wu[3]

[1]Department of Chemical and Materials Engineering, National Chin-Yi University of Technology, Taiping, Taichung, Taiwan
[2]General Education Center, Jen-Teh Junior College of Medicine, Nursing and Management, Houlong, 356, Miaoli County, Taiwan
[3]Material Application Center, Industrial Technology Research Institute, Tainan, Taiwan
Correspondence to: P.-A. Tsai (E-mail: t920402@yahoo.com.tw) or J.-H. Wu (E-mail: george6916@yahoo.com.tw)

ABSTRACT: The high/low refractive index organic/inorganic antireflective (AR) hybrid polymers were formed using the sol–gel process, in which TiO_2/2-hydroxyethyl methacrylate (2-HEMA) (high refractive index hybrid polymer) and SiO_2/2-HEMA (low refractive index hybrid polymer) two-layer thin films were formed on a hard coating deposited poly(methyl methacrylate) (HC-PMMA) substrate by both spin coating and dip coating. The relationship between the process parameters and the optical properties, thickness, porosity, surface morphology, and adhesion was determined. The results show that the reflectance of the two-layer thin films on HC-PMMA substrate is less than 0.21% ($\lambda = 550$ nm), with good adhesion (5B) and a hardness of up to 4H. In addition, the thickness, porosity, and roughness of the films affect refractive index and the antireflection properties of the AR two-layered thin film. © 2013 Wiley Periodicals, Inc. J. Appl. Polym. Sci. 000: 000–000, 2013

KEYWORDS: applications; coatings; films

Received 27 August 2012; accepted 27 December 2012; published online
DOI: 10.1002/app.38975

INTRODUCTION

It is crucial to improve the function and properties of the surface of optical materials. Coating an antireflective (AR) film on optical materials reduces reflection and increases transmission. An AR film is an interference mechanism for optical components[1] that is coated onto one or more optical thin films.[2] If the optical thickness (refraction index × thickness of the coating film) is maintained at an odd-numbered wavelength of $1/4\lambda$ of the incident wave, the reflected light experiences destructive interference. A display device with this AR film exhibits better contrast, color, and resolution.

AR films are extensively applied as semiconductors, lasers, optical magnifiers and solar cells,[3] and in the displays of everyday appliances, such as cameras, glasses, PCs, auto navigation systems,[4] large thin film transistor liquid crystal displays (TFT-LCD) and liquid-crystal display televisions (LCD-TV), cell phones, and personal digital assistants (PDA).

AR films can be prepared by vacuum deposition, chemical vapor deposition, dipping,[5] spinning, and roll-to-roll wet coating and by electron beam or the use of erosive solution technology. The principle is that when the incident light passes through the film coating, it generates transmitted and reflected light. The reflected light interferes with transmitted light of a particular wavelength in the multilayer thin film structure, which causes an optimal degree of antireflection in the range of visible light.

This study produces hybrid materials[6,7] with high/low refractive index, using the sol–gel process, which is a low cost and easy to use method for large display panels. Although the antireflection coatings (SiO_2/TiO_2) with porous structure has been investigated for a long time, no study about optimized process conditions of antireflection coatings on PMMA substrate has been found. The objective of this study was to characterize the optical properties, thickness, porosity, surface morphology, and adhesion of the AR thin films, as influenced by spin coating and dip coating under various conditions.

EXPERIMENTAL

Synthesis of High Refractive Index Hybrid Material

First, titanium (IV) *n*-butoxide (TBOT, 99%; ACROS) and acetylacetone (AcAc; Wako Pure Chemical Industry Co., Japan) were dissolved, using 2-propanol (IPA; Kanto Chemical Co.) in a reactor in which a catalyst of hydrochloric acid (HCl), distilled water, and IPA were proportionally mixed. This mixture was dropped via a separator funnel into the reactor, in order to control the speed of hydrolysis of the titanium alkoxides. After 5 h of reaction, the molar ratio of each was TBOT : AcAc :

Table I. Transmission (Tt%) of Two Thin Films Arranged with Different Spin Coating Rate of TiO_2/2-HEMA and SiO_2/2-HEMA Layer Using a Spin Coating Method on HC-PMMA

Spin coating rate (rpm)		SiO_2/2-HEMA layer				
		5000	4000	3000	2000	1000
TiO_2/2-HEMA layer	5000	93.27	94.57	95.25	95.24	92.02
	4000	93.71	93.64	94.38	95.21	93.06
	3000	93.59	95.15	94.97	95.51	93.67
	2000	93.21	94.98	94.63	95.46	92.18
	1000	95.53	95.69	95.35	94.20	92.94

H_2O : HCl : IPA = 1 : 1 : 4 : 4 : 4. UV-type organic phase of 2-hydroxyethyl methacrylate (2-HEMA; Kanto Chemical Co.) was then stirred into the mixture for 1 h, at room temperature. TiO_2 was incorporated into HEMA which is 10 wt %. The concentration of the solution for the coating is 4–5%. Finally, photoinitiator (benzophenone) will be added into the mixture for 30 min.

Synthesis of Low Refractive Index Hybrid Material

First, tetraethyl orthosilicate (TEOS, 98%, ACROS) precursor was placed into a reactor, along with HCl, IPA, and distilled water in a molar ratio of 1 : 4 : 4 : 4, for 5 h at a reaction temperature of 60°C. UV-type 2-HEMA was then stirred into the mixture for 1 h, at room temperature. SiO_2 was incorporated into HEMA which is 10 wt %. The concentration of the solution for the coating is 4–5%. Finally, photoinitiator (benzophenone) will be added into the mixture for 30 min.

Process of Two-Layer AR Film

First, the hard coating poly(methyl methacrylate) substrate (HC-PMMA, hardness is 4H; Entire Technology Co.) was cleaned, using IPA. The highly reflective hybrid material (TiO_2/2-HEMA) was then coated onto the PMMA substrate, using a spin coating method or a dip coating method, using specific coating parameters. The coating was then UV cured (300 Win^{-1}; Fusion UV System, Inc., USA) followed by thermal treatment at 100°C for 1 h. The SiO_2/2-HEMA for the second layer was coated onto the highly reflective hybrid material layer, using other specific coating parameters, by spin coating or dip coating. The SiO_2/2-HEMA layer was then UV cured (300 Win^{-1}; Fusion UV System, Inc., USA) followed by thermal treatment at 100°C for 1 h.

Experimental Instruments

This study used a UV–vis (Varian Cary 100), a Spectro Ellipsometer (J.A. Woollam M2000), a haze meter (Haze; Model NDH-2000), a Contact Angle and Surface Energy meter (FTA136), a hardness pencil test (LT-291), Adhesion Cross-Cut Testers (Adhesion: slsl-600), an Atomic Force Microscope (P47-PRO), and FE-SEM (S-4000).

RESULTS AND DISCUSSION

Transmission Properties of AR Two-Layered Film

The organic/inorganic hybrid materials were coated onto HC-PMMA using spin coating, with a different spin coating rate for TiO_2/2-HEMA and SiO_2/2-HEMA. Table I shows that the two layers produced at a spin coating rate of 1000 rpm (TiO_2/2-HEMA) and 4000 rpm (SiO_2/2-HEMA) have much better transmission (Tt% = 95.69%). Hence, this study used a spin coating rate of 1000 rpm for TiO_2/2-HEMA coating and 1000–5000 rpm for SiO_2/2-HEMA coating.

The other coating method involved coating the organic/inorganic hybrid materials onto HC-PMMA using dip coating with a different withdrawal rate. Table II shows that two layers produced at a withdrawal rate of 4.0 mm/s (TiO_2/2-HEMA) and 2.2 mm/s (SiO_2/2-HEMA) exhibit good transmission (Tt% = 99.35%). This study used a withdrawal rate of 4.0 mm/s for TiO_2/2-HEMA coating layer and 2.2–4.0 mm/s for SiO_2/2-HEMA coating layer, for dip coating. A comparison with Tables I and II show that the two layers produced by dip coating have better transmission than those produced by spin coating method.[8]

The Refractive Index of AR Two-Layered Film

Figures 1 and 2 show the refractive indices of the thin film are inversely proportional to wavelength. This behavior has also been noted in literature.[9] Figure 1 also shows that the refractive index of the SiO_2/2-HEMA film is inversely proportional to the spin coating rate, but Figure 2 shows that the refractive index of the SiO_2/2-HEMA layer is directly proportional to the withdrawal rate for the dip coating method.

Table II. Transmission (Tt%) of Two Thin Films Arranged with Different Withdrawal Rate of TiO_2/2-HEMA and SiO_2/2-HEMA Layer on HC-PMMA Using a Dip Coating Method

Withdrawal rate (mm/s)		SiO_2/2-HEMA layer					
		2.2	2.5	3.0	3.2	3.7	4.0
TiO_2/2-HEMA layer	2.2	97.84	98.82	99.10	98.84	97.18	96.21
	2.5	97.99	99.10	99.23	98.75	96.83	95.23
	3.0	98.48	99.07	99.05	98.39	96.31	94.29
	3.2	99.18	98.97	98.57	98.18	95.65	94.22
	3.7	99.10	98.84	98.30	98.03	95.39	92.96
	4.0	99.35	98.63	98.21	97.42	94.07	93.06

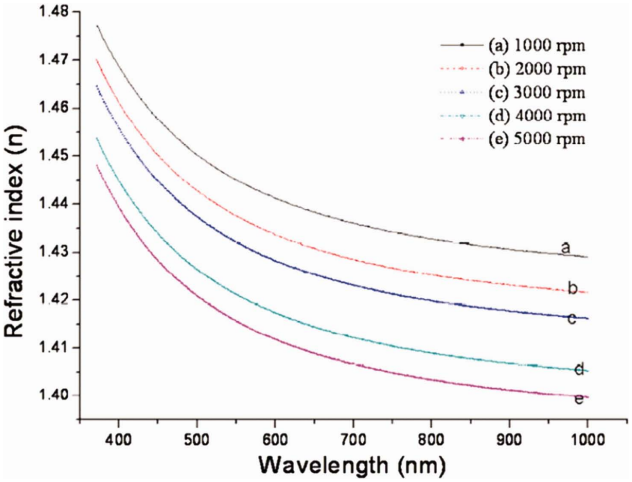

Figure 1. The refractive index for different spin coating rates onto HC-PMMA at the SiO_2/2-HEMA layer, using the spin coating method (TiO_2/2-HEMA layer = 1000 rpm). [Color figure can be viewed in the online issue, which is available at wileyonlinelibrary.com.]

Thickness of AR Two-Layered Film

It is important to control the thin film thickness for an AR coating, because its reflectivity is affected by the film's thickness and refractive index. Figure 3 shows that the spin coating rate can be used to control the thickness of the film on HC-PMMA. The thickness of thin film coating is inversely proportional to the spin coating rate.[10]

The dip coating method can produce dual properties; this is the major difference[11] between spin coating and dip coating. Figure 4 shows that the thickness of the thin film coatings is proportional to the withdrawal rate used for the dip coating method, which is also noted in literature.[12,13] Furthermore, as shown in Figures 5 and 6, the thickness of films produced by dip coating is directly related to the reflectance (R%) but exhibits an inverse relationship with the transmission (Tt%)[14] on HC-PMMA substrate.

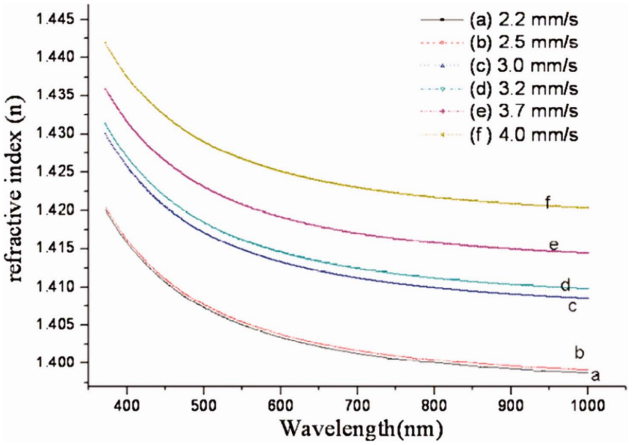

Figure 2. The refractive index for different withdrawal rates for HC-PMMA at the SiO_2/2-HEMA layer, using the dip coating method (TiO_2/2-HEMA layer = 4.0 mm/s). [Color figure can be viewed in the online issue, which is available at wileyonlinelibrary.com.

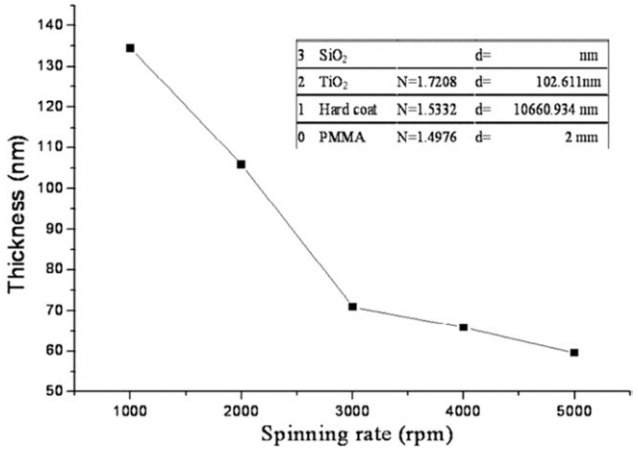

Figure 3. The film thickness as a function of the spin coating rate onto HC-PMMA at the SiO_2/2-HEMA layer, using the spin coating method (TiO_2/2-HEMA layer = 1000 rpm).

Figure 7 shows that when the HC-PMMA with an optical coating is observed from a certain angle, its reflex contains different colors. For example, Figure 7(c) shows a pink–purple color on the thin film coatings, which could be an AR effect.[15] In Figure 7(d), intense reflex can be seen for the uncoated PMMA substrate. Different film thicknesses eliminate the different reflexes of various frequencies. This effect can offset a certain wavelength of the reflex, so the color of the reflex varies accordingly.

Surface Contact Angle and Surface Energy of AR Two-Layered Film

Table III shows that as the spin coating rate increases, the surface contact angle decreases and the surface energy increases, for two-layer optical film coatings on HC-PMMA at the SiO_2/2-HEMA layer, using the spin coating method. This result can be used to improve the properties of the contact angle and surface energy of the HC-PMMA at the SiO_2/2-HEMA layer. Table IV shows that the surface contact angle is directly related to and

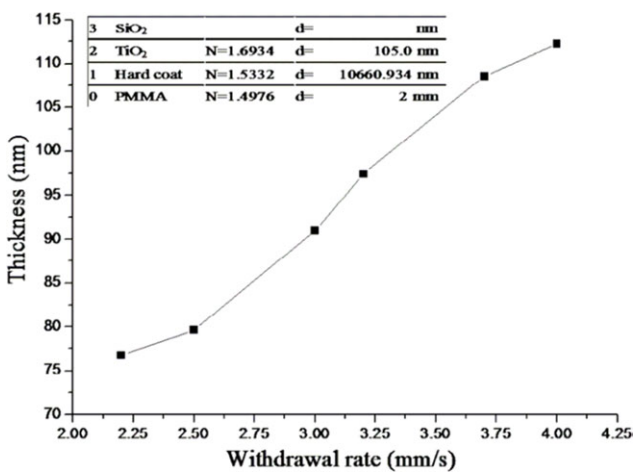

Figure 4. The film thickness as a function of the withdrawal rate of HC-PMMA at the SiO_2/2-HEMA layer, using the dip coating method (TiO_2/2-HEMA layer = 4.0 mm/s).

Applied Polymer SCIENCE

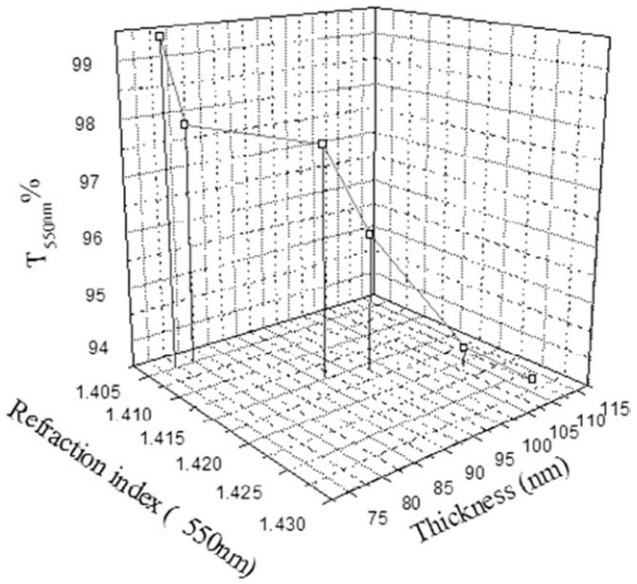

Figure 5. Transmission (Tt%) as a function of refractive index and thickness at λ = 550nm, using the dip coating method (TiO_2/2-HEMA layer = 4.0 mm/s).

the surface energy are inversely related to the withdrawal rate of the HC-PMMA at the SiO_2/2-HEMA layer, using the dip coating method.

Atomic force microscopy (AFM) and scanning electron microscopy (SEM) were used to observe the surface morphology of the thin film coatings. Figure 8 shows the AFM 3D surface images of HC-PMMA at the SiO_2/2-HEMA layer, produced by the dip coating method. AFM analysis allows the determination of the surface stereostructure and roughness value (Ra) of the thin film coatings. It also shows that the distribution of poles

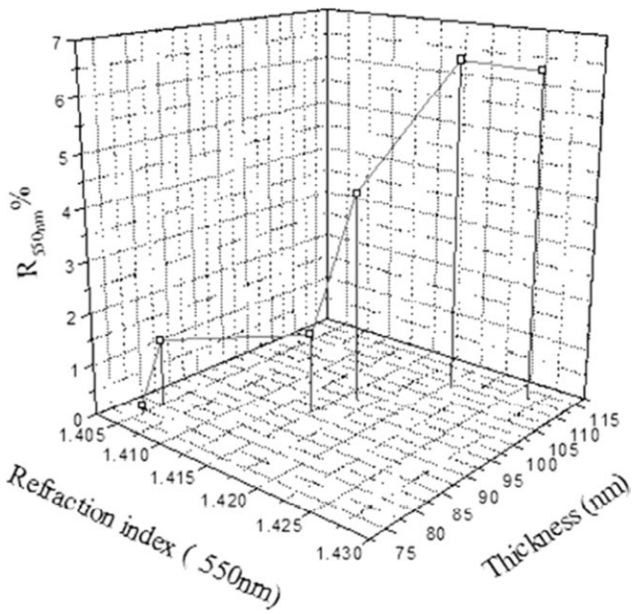

Figure 6. Reflectance (*R*%) as a function of refraction index and thickness at λ = 550 nm, using the dip coating method (TiO_2/2-HEMA layer = 4.0 mm/s).

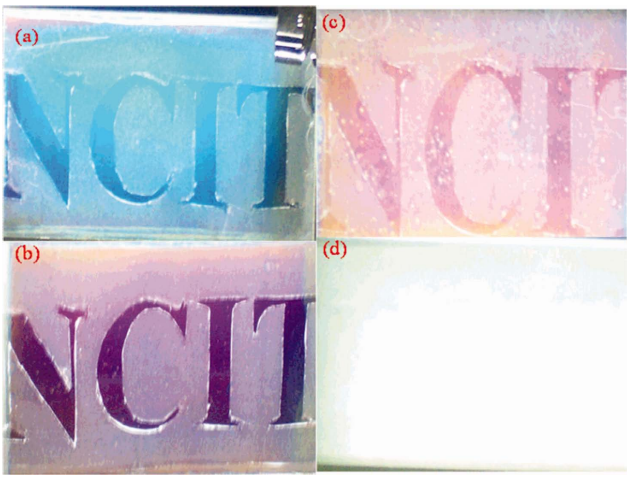

Figure 7. Demonstration of AR effect of a coating on a HC-PMMA, using the dip coating method (λ = 550nm): (a): *T*% = 95–98%, *R*% = 2–5%, (b) *T*% = 98–99%, *R*% = 1–2%, (c) *T*% = 99%, *R*% = 1%, and (d) *T*% = 91.8%, *R*% = 8.2% (uncoated substrate). [Color figure can be viewed in the online issue, which is available at wileyonlinelibrary.com.

on the surface of thin film coatings decreases, when the withdrawal rate is increased.

Figure 9(a–f) shows the SEM images (10,000 times) of HC-PMMA at the SiO_2/2-HEMA layer, for various withdrawal rates. Obviously, the distribution of poles on the surface of the thin film coatings decreases,[16] as the withdrawal rate is increased.

Both AFM and SEM show that some poles exist on the surface of the thin film coatings.[12,16–18] The phenomenon of organic/inorganic hybrid materials with poles was noted by researchers in 1980.[19,20] The porosity of the thin film coatings is determined using the following formula[21]:

$$\text{Porosity} = \left(1 - \frac{n^2 - 1}{n_d^2 - 1}\right) \times 100(\%) \quad (1)$$

where n_d is the refractive index (n_d = 1.45) of pure SiO_2/2-HEMA at a wavelength of 550 nm and n is the refractive index of the optical thin film coating with poles, at the same wavelength (550 nm).

Table III. The Contact Angle and Surface Energy with Different Spin Coating Rate on HC-PMMA at SiO_2/2-HEMA Layer Using a Spin Coating Method

Materials	Spin coating rate (rpm)	Contact angle (°)	Surface energy (dy/cm^2)
TiO_2/2-HEMA and SiO_2/2-HEMA layer	1000-1000	95.54	14.86
	1000-2000	92.43	16.72
	1000-3000	84.40	21.93
	1000-4000	83.16	22.81
	1000-5000	83.13	22.84
HC-PMMA	-	41.58	55.59

Table IV. The Contact Angle and Surface Energy with Different Withdrawal Rate on HC-PMMA at SiO_2/2-HEMA Layer Using a Dip Coating Method

Materials	Withdrawal rate (mm/s)	Contact angle (°)	Surface energy (dy/cm^2)
TiO_2/2-HEMA and SiO_2/2-HEMA layer	4.0–2.2	81.63	23.89
	4.0–2.5	85.09	21.39
	4.0–3.0	86.38	20.57
	4.0–3.2	88.73	19.03
	4.0–3.7	89.54	18.50
	4.0–4.0	90.81	17.70
HC-PMMA	-	41.58	55.59

Table V shows that the porosity and roughness of the thin film coatings are inversely related to the withdrawal rate of the HC-PMMA at the SiO_2/2-HEMA layer, using the dip coating method. Figure 10 shows that a decrease in porosity results in a higher refractive index for the thin film coatings at the SiO_2/2-HEMA layer. Other studies[22] have also shown that porous sol–gel thin films show increased transmission (Tt%) and reduced reflectance (*R*%). Therefore, the distribution of poles can be used to control the refractive index and to produce antireflection films.[23] The distribution of poles is related to the viscosity, surface energy, and the coating rate of the substrates.[24] A solvent mixture with a different boiling point and close control of the rise in temperature in the oven could cause a decrease in the distribution of poles.

Hardness and Adhesion Properties of AR Two-Layered Film

Hardness and adhesion are essential properties for thin film coatings. Table VI shows the hardness results for HC-PMMA substrates produced by dip coating. This test is applied to understand hardness of the surface. The pencils with rated hardness from 6H to 6B (hard to soft) were tested, starting with hardness 6H and proceeding down one level of hardness, until one pencil was found that could not make a scratch on the substrate. Since materials with high/low refraction index are processed onto nanoscale thin films by the sol–gel process, the hardening layer gives the film coatings on the HC-PMMA a hardness of as much as 4H. Table VI also shows the adhesion[11] between each layer, which was analyzed by a crosscut tester. The films were cut through in six lines (1 mm spacing). This cutting guide was then rotated 90° and another six lines were cut through the film, leaving behind a grid with 25 squares. Standard pressure-sensitive tape was applied to the grid and removed evenly within 5 min of applying the tape. In this study, good adhesion was achieved, from the HC-PMMA through the hardening layer, the high refractive index TiO_2/2-HEMA layer, and the low refractive index SiO_2/2-HEMA layer, all of which demonstrated an adhesion testing of 5B.

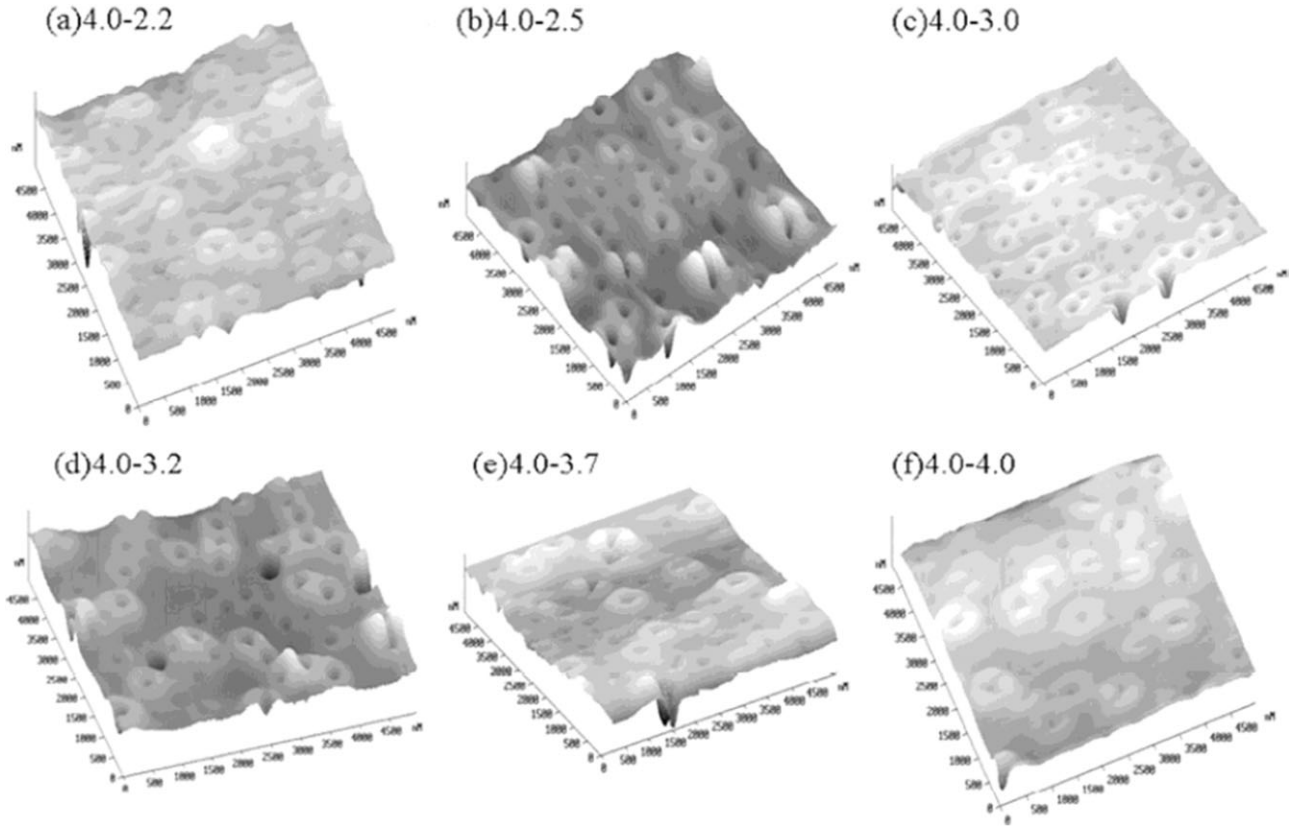

Figure 8. AFM 3D images of two layer-coated thin film with different withdrawal rates (2.2–4.0 mm/s) at the SiO2/2-HEMA layer on HC-PMMA, using a dip coating method (TiO_2/2-HEMA layer = 4.0 mm/s).

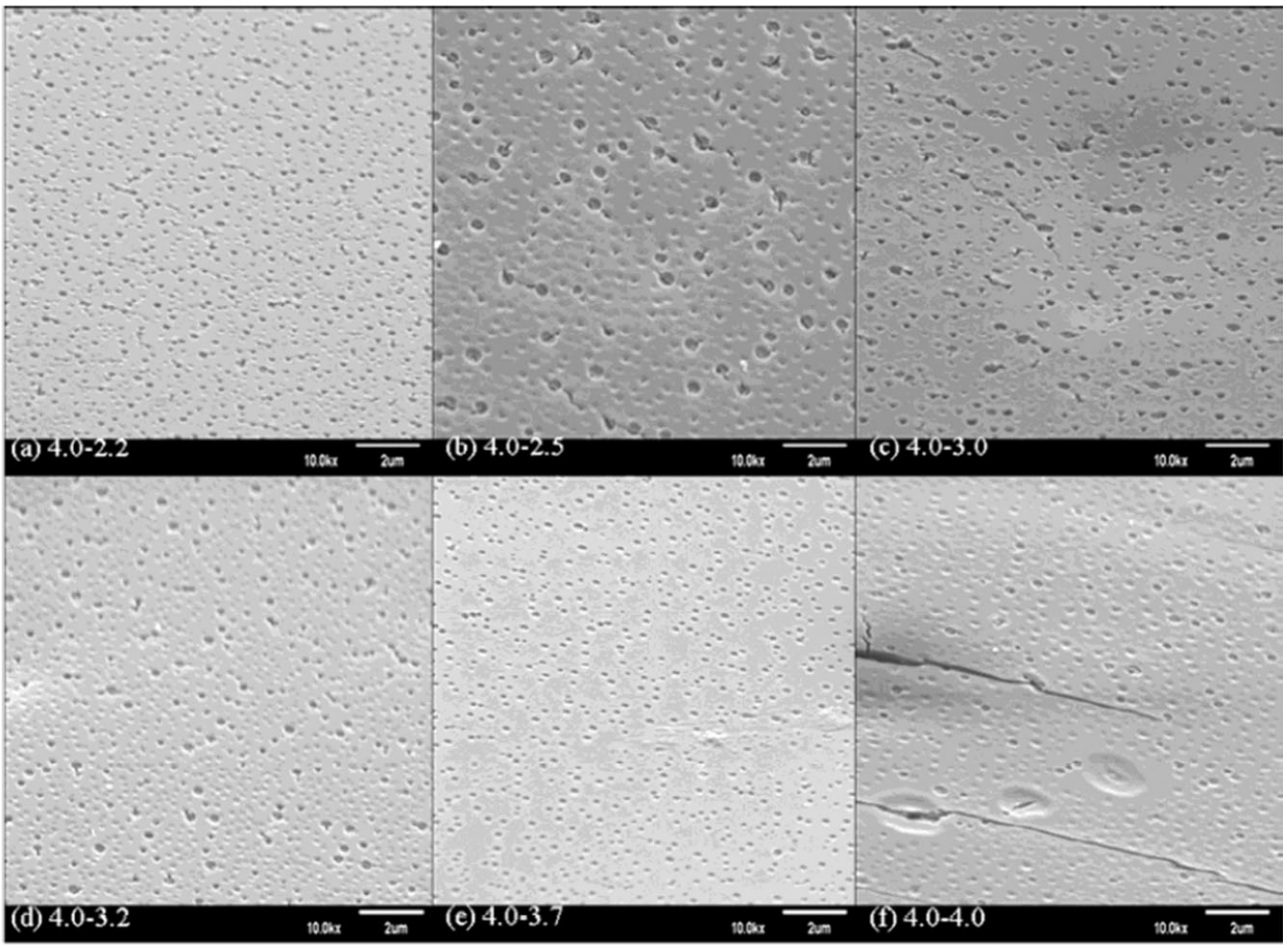

Figure 9. SEM images of two layer-coated thin film with different withdrawal rates (2.2–4.0 mm/s) at the SiO_2/2-HEMA layer on HC-PMMA, using a dip coating method (TiO_2/2-HEMA layer = 4.0 mm/s).

CONCLUSIONS

This study produced organic/inorganic hybrid materials, using a wet sol–gel process. The materials were coated onto HC-PMMA, using spin coating and dip coating methods, after UV curing, to produce a two-layer optical thin film coating.

The results of this study show that the film thickness is inversely proportional to the rotational speed used for the spinning coating method but directly proportional to the withdrawal rate used for the dip coating method. The porosity of the surface of the thin film coatings is inversely proportional to the refractive index but directly proportional to the surface energy.

Table V. The Porosity and Surface Roughness (Ra) with Different Withdrawal Rate on HC-PMMA at SiO_2/2-HEMA Layer Using a Dip Coating Method

Materials	Withdrawal rate (mm/s)	Porosity (%)	Surface roughness (nm)
TiO_2/2-HEMA and SiO_2/2-HEMA layer	4.0-2.2	11.65	13.98
	4.0-2.5	11.55	15.82
	4.0-3.0	9.12	21.36
	4.0-3.2	8.78	26.42
	4.0-3.7	7.60	33.32
	4.0-4.0	6.07	34.65

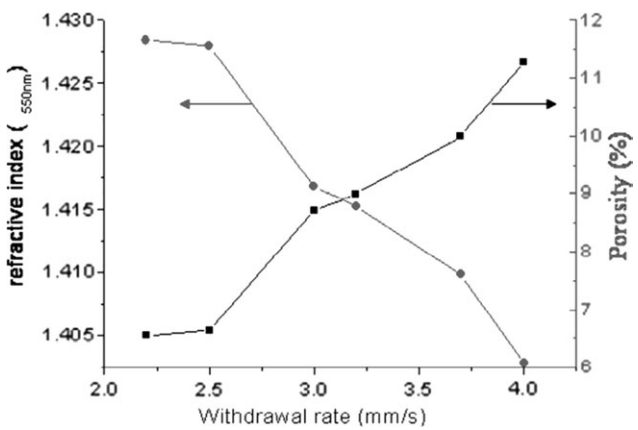

Figure 10. Refractive index and porosity as a function of withdrawal rate (2.2–4.0 mm/s) at the SiO_2/2-HEMA layer on HC-PMMA, using a dip coating method (TiO_2/2-HEMA layer = 4.0 mm/s).

Table VI. The Pencil Hardness and Adhesion Property with Different Withdrawal Rate on HC-PMMA at SiO_2/2-HEMA Layer Using a Dip Coating Method

Materials	Withdrawal rate (mm/s)	Hardness[a]	Adhesion test[b]
TiO_2/2-HEMA and SiO_2/2-HEMA layer	4.0–2.2	4H	5B
	4.0–2.5	4H	5B
	4.0–3.0	4H	5B
	4.0–3.2	4H	5B
	4.0–3.7	4H	5B
	4.0–4.0	4H	5B

[a]ASTM D3363-74: the pencils with rated hardness from 6H to 6B (hard to soft). The hardness rating of the final test pencil was defined as the hardness of the coatings.
[b]ASTM D3359-78: The classification of adhesion test result is 0B when over 65% flaking of the crosscut area is occurred and 5B when no flaking is observed. The degree of 1–4B was determined between 0B and 5B.

In two-layer optical mechanisms, low refractive index SiO_2/2-HEMA varies with thickness, depending on the various refractive indices. As a result, greater optical thickness results in high reflectance and low transmission.

The experimental data show that the best withdrawal rate for high/low refractive materials (TiO_2/2-HEMA???SiO_2/2-HEMA), using the dip coating method for HC-PMMA, is 4.0 mm/s for the TiO_2/2-HEMA layer and 2.2 mm/s for the SiO_2/2-HEMA layer. This prevents refection through interference light and produces a thin film coating with reduced AR properties ($R\%_{550\ nm} = 0.21\%$) and high transmission ($Tt\%_{550\ nm} = 99.33\%$). In addition, the adhesion between each layer of the two-layer optical thin films are good (5B) and the hardness is as much as 4H.

REFERENCES

1. Que, W.; Hu, X. *Opt. Mater.* **2003**, *22*, 31.
2. Shanbhogue, H. G.; Prasad, S. N.; Nagendra, C. L.; Thutupalli, G. K. M. *Thin Solid Films* **1998**, *320*, 290.
3. Bouhafs, D.; Moussi, A.; Chikouche, A.; Ruiz, J. M. *Sol. Energy Mater. Sol. Cells* **1998**, *52*, 79.
4. Chen, D.; Yan, Y.; Westenberg, E.; Niebauer, D.; Sakaitani, N.; Chaudhuri, S. R.; Sato, Y.; Takamatsu, M. *J. Sol-Gel Sci. Technol.* **2000**, *19*, 77.
5. Notell, P.; Roos, A.; Karlsson, B. *Thin Solid Films* **1999**, *351*, 170.
6. Chiu, W. M.; Yang, C. F.; Chao, Y. H. *J. Appl. Polym. Sci.* **2007**, *103*, 2271.
7. Chiu, W. M.; Yang, C. F.; Zhang, Y. S. *Polym. Plast. Technol. Eng.* **2007**, *46*, 767.
8. Jiang, H.; Yu, K.; Wang, Y. *Opt. Lett.* **2007**, *32*, 575.
9. Ghodsi, F. E.; Tepehan, F. Z. *Thin Solid Films* **1997**, *295*, 11.
10. Morford, P. V.; Mercado, R. L.; Planje, C. E.; Flaim, T. D. *Proc. SPIE* **2005**, *5724*, 34.
11. Chen, D. *Sol. Energy Mater. Sol. Cells* **2001**, *68*, 313.
12. Vicente, G. S.; Morales, A.; Gutierrez, M. T. *Thin Solid Films* **2001**, *391*, 133.
13. Vong, M. S. W.; Sermon, P. A. *Thin Solid Films* **1997**, *293*, 185.
14. Zhang, Y.; Raman, N.; Bailey, J. K.; Brinker, C. J.; Crooks, R. M. *J. Phys. Chem.* **1992**, *96*, 9098.
15. Prevo, B. G.; Hwang, Y.; Velev, O. D. *Chem. Mater.* **2005**, *17*, 3642.
16. Park, M. S.; Lee, Y.; Kim, J. K. *Chem. Mater.* **2005**, *17*, 3944.
17. Kim, D. J.; Hahn, S. H.; Oh, S. H.; Kim, E. J. *Mater. Lett.* **2002**, *57*, 355.
18. Das, S.; Roy, S.; Patra, A.; Biswas, P. K. *Mater. Lett.* **2003**, *57*, 2320.
19. Loy, D. A.; Shea, K. J. *Chem. Rev.* **1995**, *95*, 1431.
20. Loy, D. A.; Jamison, G. P.; Baugher, B. M.; Russick, E. M.; Assink, R. A.; Prabakar, S.; Shea, K. J. *J. Non-Cryst. Solids* **1995**, *186*, 44.
21. Yoldas, B. E. *Appl. Opt.* **1980**, *19*, 1425.
22. Gombert, A.; Glaubitt, W.; Rose, K.; Dreibholz, J.; Blasi;B.; Heinzel, A.; Sporn, D.; Doll, W.; Wittwer, V. *Sol. Energy* **2000**, *68*, 357.
23. Peeters, M. P. J.; Bohmer, M. R. *J. Sol-Gel Sci. Technol.* **2003**, *26*, 57.
24. Gutoff, E. B.; Kendrick, C. E. *AIChE J.* **1982**, *28*, 459.